

# Structural changes to a turbulent boundary layer grazing a compliant panel

By D. Bodony†

Recent direct numerical simulations of a Mach 2.25 turbulent boundary layer over a compliant surface revealed changes in the turbulent Reynolds stresses relative to a rigid-wall boundary layer. This report focuses on a computational study to determine whether a linearized model can be used to describe the changes. The simulation data suggest that the boundary-induced motion is greatly amplified by the non-uniform mean flow to levels that are more realistic than what is predicted by a uniform mean.

---

## 1. Introduction

High speed flight ( $M_\infty \geq 5$ ) is accompanied by severe thermal and fluid dynamic loads. A hypersonic vehicle will be partially wetted by a turbulent boundary layer that produces significant static and dynamic pressure and thermal loads over the majority of the outer skin. Furthermore, such a vehicle requires a powerful propulsion system, which increases the severity of the loading in the engine inlet and exhaust regions; shock impingement may also occur with a local load intensification. In order for this class of vehicle to be technologically and economically feasible, it must be lightweight, flexible, and reusable, which shrinks the design margin envelope. The intersection of the extreme environment and stringent design requirements leads to situations where structural compliance and fluid-structure interaction become significant. Large thermoacoustic loads and unknown, interaction induced-loading scenarios significantly increase the danger of fatigue. Common assumptions (e.g., structural rigidity, inviscid flow) used in design today are not valid in this regime.

Few on-ground experiments focused on high-speed fluid-structure interaction have been conducted, such as those by Glass & Hunt (1986, 1988) that involve aerothermal interaction (rigid structure), and the discovery experiments by Bebernis *et al.* (2011) of a Mach 2 flow past a thin aluminum panel in the RC19 facility at Wright-Patterson AFB. Recent investigations by McKeon and co-workers (Jacobi & McKeon 2011*a,b*; McKeon *et al.* 2013) of fluid-structure interaction focused on the response of boundary layer turbulence caused by kinematic roughness. The data indicate the presence of so-called internal layers, distinct from the critical layer from flow stability regions, that denote borders between zones containing reduced or excess amounts of turbulent fluctuation levels, relative to smooth wall boundary layers, and changes in the turbulence integral length scales. Using non-modal analysis of the locally-parallel Orr-Sommerfeld operator, McKeon and co-workers argue that a large portion of the phase-averaged changes they measure is linked to transient growth of disturbances initiated by the dynamic roughness that evolve on the turbulent mean velocity profile. This identification, plus related work on viewing turbulence generation as a continuous transient growth process, has led to possible dynamic roughness control ideas by McKeon *et al.* (2013).

† Department of Aerospace Engineering, University of Illinois at Urbana-Champaign

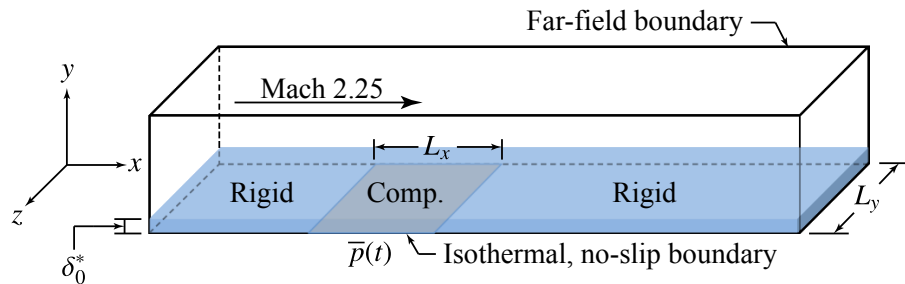


FIGURE 1. Coupled simulation domain. Streamwise  $x$  and spanwise  $z$  boundaries are periodic. “Comp.” denotes compliant.

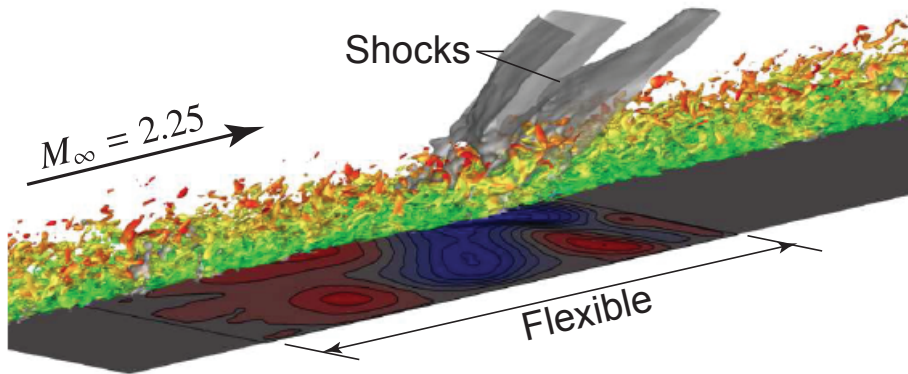


FIGURE 2. Visualization of the boundary layer vorticity (color), pressure iso surfaces (gray), and panel deformation (contour) caused by a Mach 2.25 turbulent boundary layer grazing a deformable panel.

Static roughness elements of different shapes have been specifically constructed to understand how local flow distortions can enhance or suppress turbulence production at high-speed conditions (Ekoto *et al.* 2008, 2009). It was identified that sufficiently strong roughness-induced local flow expansions can lead to turbulence suppression through a reorganization of the turbulence production tensor and, with it, the pressure-strain redistribution. Although static these measurements are useful in the dynamic case, whether one can treat panel deformations as quasi-static and draw analogies between dynamic and static roughness is currently unknown.

The lack of experimental and numerical data on turbulent boundary layer-panel interaction leads to an uncertainty in our understanding of their coupling and how changes to canonical turbulent boundary layers, if they exist, must be incorporated using reduced-fidelity models. The purpose of this work is to improve our understanding and modeling of turbulent boundary layers flowing adjacent to compliant surfaces by analyzing existing numerical databases. Details of the databases are given in Section 2, followed by our approach and results in Sections 3 and 4, respectively.

## 2. Original direct numerical simulation database

A series of direct numerical simulations of a temporally-developing Mach 2.25 turbulent boundary layer were conducted adjacent to a deformable, but not thermally-conducting,

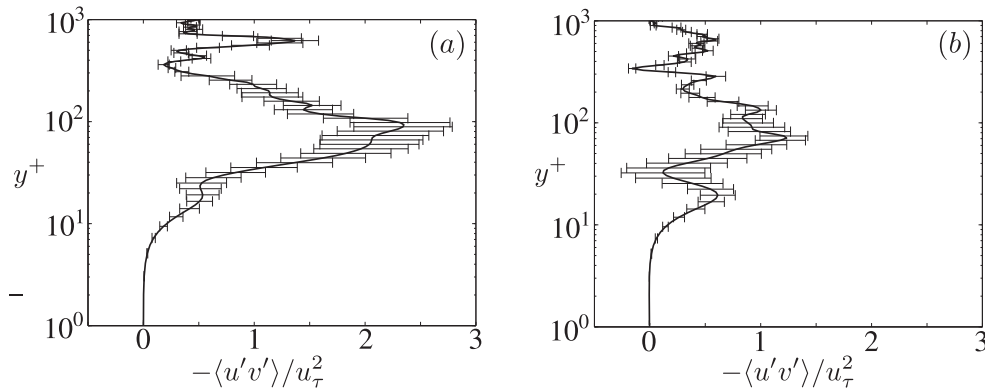


FIGURE 3. Primary Reynolds stress  $\langle u'v' \rangle / u_\tau^2$  of the turbulent boundary layer immediately above the panel for a rigid (a) and dynamic panel taken at the moment of maximum deflection out of the boundary layer (b). Observe the reduction in the Reynolds stress.

metallic panel as depicted in Figure 1, with simulation image given in Figure 2. The objective was to investigate, from first principles, the interaction of moderately-compressible turbulence with a compliant surface to understand changes to the turbulence and identify failings of commonly-used reduced order models. The minimum momentum-thickness-based Reynolds number was approximately 1,500 for the fully turbulent boundary layers. Details on the boundary layer validation and numerical methods used are given in Ostoich *et al.* (2013).

The thin panel chosen fluttered and was found to generate a strong acoustic field, though weak by shock standards, that appeared as coherent oblique waves whose position over the panel followed the panel deformation (Figure 2). After an initial transient period the panel settled into a nonlinear limit cycle oscillation with panel deflections that approached  $25^+$  wall units into and out of the boundary layer. Statistical data showed the turbulence structure was altered by the panel motion and resulted in either a reduction of turbulence production (Figure 3) when the panel deflection was away from the flow, similar to the findings of Ekoto *et al.* (2009), but without obvious turbulence production enhancement when the panel deflected into the flow (not shown). An analysis of the turbulence downstream of the panel and over a rigid portion showed that, based on a turbulence kinetic energy budget, the non-equilibrium turbulence relaxed to its smooth, rigid wall form within one integral turbulence length scale.

The observed modification of the dominant Reynolds stress in Figure 3 suggested that reduced-order models frequently used to estimate the performance characteristics of flight vehicles, such as Reynolds-averaged Navier-Stokes (RANS) approaches, may need corrections to account for the compliancy of the adjacent surface. The purpose of this work was to understand whether a linear model would be sufficient to account for these effects. In essence this report documents an investigation to understand whether a linear model is sufficient to predict the changes in  $\langle u'v' \rangle$ , for example.

### 3. Approach

The observation that surface compliance modifies the underlying turbulent structure can be viewed as a perturbation problem where the turbulence that would normally be present over a rigid surface is altered by an amount that depends on the surface

motion. There are many ways to view this perturbation but, for this work, we assume that a simple additive change is sufficient and try to determine whether this is true. For example, we assume that a velocity fluctuation,  $u'$ , is comprised as the sum of a rigid component and a correction,

$$u' = u'_{\text{rigid}} + u'_{\text{compliant}} \quad (3.1)$$

where  $u'_{\text{compliant}}$  is assumed to be associated with the surface motion and is equal to zero if the surface is rigid. For sake of simplicity the ‘‘compliant’’ subscript is dropped so that all primed quantities are to be associated with the surface motion, unless otherwise noted. The perturbations to the density, momentum, and total energy,  $\{\rho', (\rho u_i)', (\rho E)'\}$ , are governed by

$$\frac{\partial}{\partial t} \left( \frac{\rho'}{J} \right) + \frac{\partial}{\partial \xi_j} \left( \rho' \hat{U}_j + \bar{\rho} u'_k \hat{\xi}_{j,k} \right) = 0, \quad (3.2)$$

$$\frac{\partial}{\partial t} \left( \frac{(\rho u_i)'}{J} \right) + \frac{\partial}{\partial \xi_j} \left( (\rho u_i)' \hat{U}_j + \bar{\rho} \bar{u}_i u'_k \hat{\xi}_{j,k} + p' \hat{\xi}_{j,i} \right) = \frac{\partial}{\partial x_j} \tau'_{ij}, \quad (3.3)$$

$$\begin{aligned} \frac{\partial}{\partial t} \left( \frac{(\rho E)'}{J} \right) + \frac{\partial}{\partial \xi_j} \left( [(\rho E)' + p'] \hat{U}_j + [(\bar{\rho} \bar{E} + \bar{p}) \hat{\xi}_{j,k} u'_k] - p' \hat{\xi}_{j,t} \right) &= \frac{\partial}{\partial x_j} (\bar{\tau}_{ij} u'_i + \tau'_{ij} \bar{u}_i), \\ &- \frac{\partial}{\partial x_j} \dot{q}'_j \end{aligned} \quad (3.4)$$

where  $\hat{U}_i = \hat{\xi}_{i,\tau} + \bar{u}_j \hat{\xi}_{i,j}$  is the mean contravariant velocity,  $\hat{\xi}_{i,j} = J^{-1} \partial \xi_i / \partial x_j$  is the Jacobian-weighted metric, and  $\tau'_{ij}$  and  $\dot{q}'_j$  are the linearized viscous stress tensor and heat flux vector, respectively, for a Newtonian fluid with Fourier’s law for conduction. These equations are valid in generalized curvilinear coordinates and are completed with a calorically perfect gas with equation of state,

$$p' = (\gamma - 1) \left\{ (\rho E)' - \frac{1}{2} \bar{\rho} \bar{u}_i u'_i - \frac{1}{2} (\rho u_i)' \bar{u}_i \right\} \quad (3.5)$$

with constant  $\gamma = 1.4$ . The governing equations Eqs. (3.2)–(3.4) are supplemented by the no-slip and isothermal boundary conditions as  $u'_i = \dot{x}_{w,i}$  at  $T' = 0$ , respectively, where  $\dot{x}_{w,i}$  is the wall velocity in the  $i$ th direction. The initial condition is that all perturbations are equal to zero.

Discretization of the linearized equations uses the summation-by-parts (SBP) and simultaneous-approximation-term (SAT) approach (Strand 1994; Svård *et al.* 2007; Svård & Nordström 2008) with special attention to the discretization of the metric terms to ensure satisfaction of the geometric conservation law (Visbal & Gaitonde 2002). Linearized forms for the SAT boundary terms are used and available elsewhere (Natarajan *et al.* 2014). Time integration used a standard fourth order Runge-Kutta algorithm along with the 2-4 diagonal norm SBP scheme (Strand 1994).

As the surface deforms the grid above it also deforms. If the current location of a grid point fixed to the compliant surface is  $\vec{x}_w$ , then the perturbation  $\vec{\delta} = \vec{x}_w(t) - \vec{x}_w(0)$  from the original configuration is pushed onto the fluid grid by transfinite interpolation. Because  $\vec{x}_w$  is a known function of time, the grid metrics  $\hat{\xi}_{i,\tau}$  are easily computed. The surface motion was extracted from the DNS database and stored in a file to be read in by the linearized solver.

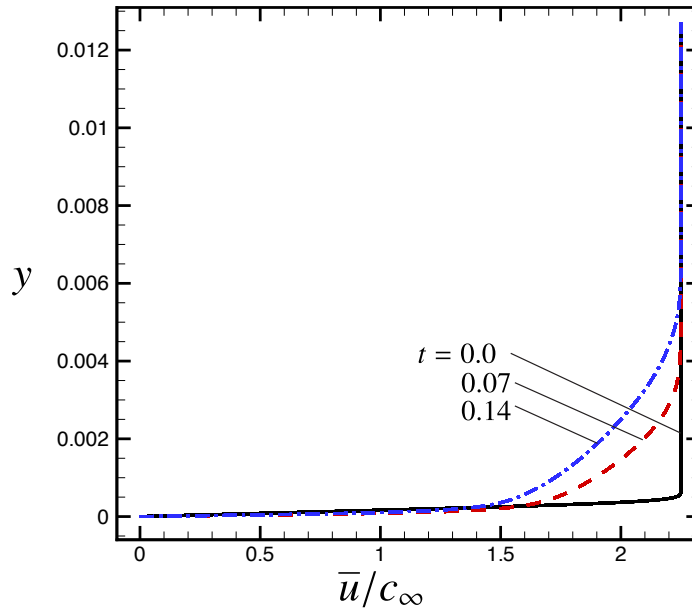


FIGURE 4. Evolution of mean streamwise velocity extracted from the DNS.

#### 4. Results

The linearized equations in Eqs. (3.2)–(3.4) require specification of the space-time dependent mean flow about which the perturbations exist. For the present work, three different mean flows were chosen: a uniform mean flow, a steady but nonuniform mean flow taken from the initial condition of the DNS where a parallel compressible Blasius boundary layer exists over an isothermal wall of temperature 322 K, and an unsteady mean flow taken from the DNS by averaging the solution in the  $x$ - and  $z$ -homogeneous directions. In all cases the free stream Mach number of the baseflow is 2.25, the ambient temperature is 322 K and, where appropriate, the wall temperature is also 322 K. The latter mean flow is a function of the wall normal coordinate  $y$  and of time  $t$ , as shown in Figure 4. Note that the mean profile at  $t = 0.0$  in Figure 4 is equivalent to the steady but nonuniform mean.

The linearized simulations proceed by reading the surface motion  $\vec{x}_w(x, z, t)$  from the precomputed DNS database and by specifying the baseflow according to the three possibilities outlined above. A visual outline of the different responses is shown in Figure 5 for the three different baseflows, taken at the same absolute time along an  $x$ - $y$  plane taken in the mid- $z$  location. The figure indicates that the choice of the baseflow has consequences on the level and type of disturbance the surface motion can introduce. In all three subfigures the acoustic field created by the surface deformation is qualitatively similar; however, the acoustic field in the uniform baseflow case shows more detail as the surface motion is more easily able to impact the fluid, whereas for the latter two images the boundary layer acts to smoothen the acoustic field. Figure 5 also shows that the surface motion can generate trapped disturbances that are confined to the boundary layer but the details of those perturbations are strongly dependent on the thickness of the boundary layer.

The importance of the mean flow is shown in Figure 6 where the disturbance kinetic

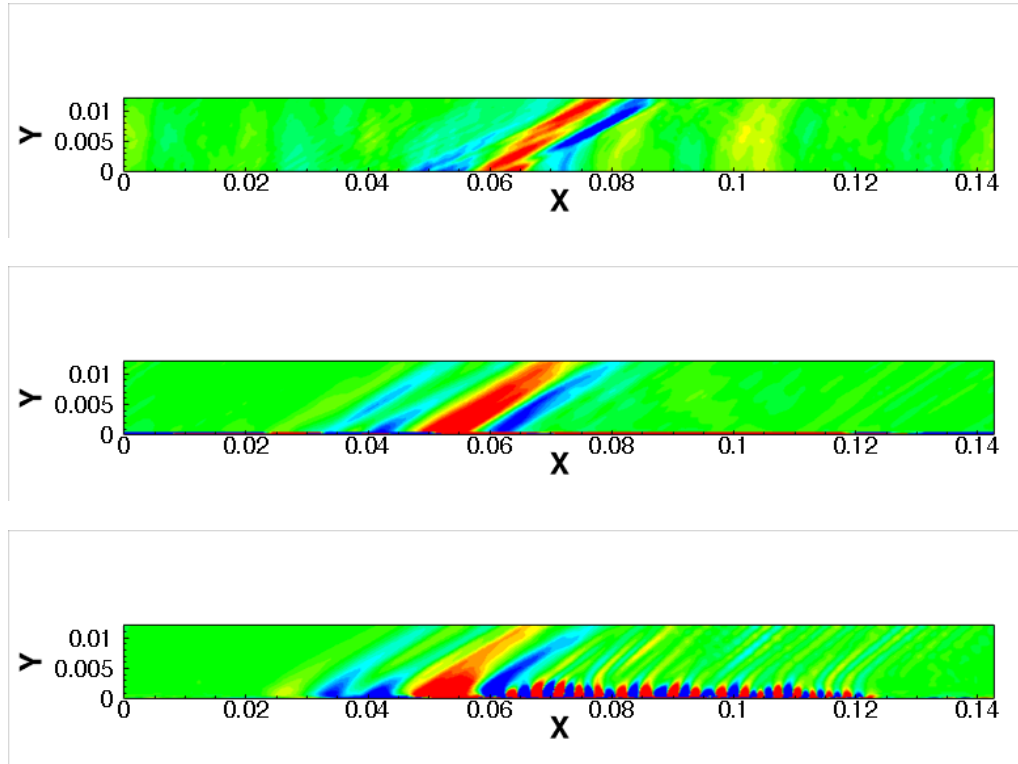


FIGURE 5. Streamwise velocity perturbation,  $u'$ , due to unsteady surface motion for uniform (top), steady but nonuniform (middle), and unsteady nonuniform (bottom) baseflows. Contour levels are different for all three figures.

energy,  $\langle u'_i u'_i \rangle / 2$ , where averaging is done in the  $x$ - and  $z$ -directions, shows a monotonic increase in the energy as the mean flow changes from uniform, to steady but nonuniform, to unsteady and nonuniform flows. The impact of the mean is dramatic. For the uniform and steady mean the wall motion induces acoustic-like disturbances that propagate away from the surface and have relatively small amplitude. However, when a nonuniform mean flow is present, the disturbances couple to it and amplify considerably through the generation of vortical disturbances. The space-time structure of the disturbances is dependent on the surface motion; the data suggest that the panel motion creates disturbances that are more able to couple the growing mean flow than they are to the steady mean flow, indicating the panel's motion may be directly tied to the growing boundary layer so that the two may not be independent.

The fact that the panel-induced motion creates disturbances that are subsequently amplified by the boundary layer suggests that modification of the turbulent structure is possible, as indicated by the original DNS data shown in Figure 3. In traditional flutter analysis, the presence of a boundary layer is typically neglected and flutter is consequently seen as a predominantly inviscid phenomenon (Dowell 1970). However, the current results suggest that the boundary layer is important as it may selectively amplify certain panel motion-induced disturbances and alter the basic structure of the turbulence within the boundary layer. However, there is a sensitivity to the mean flow on which the dis-

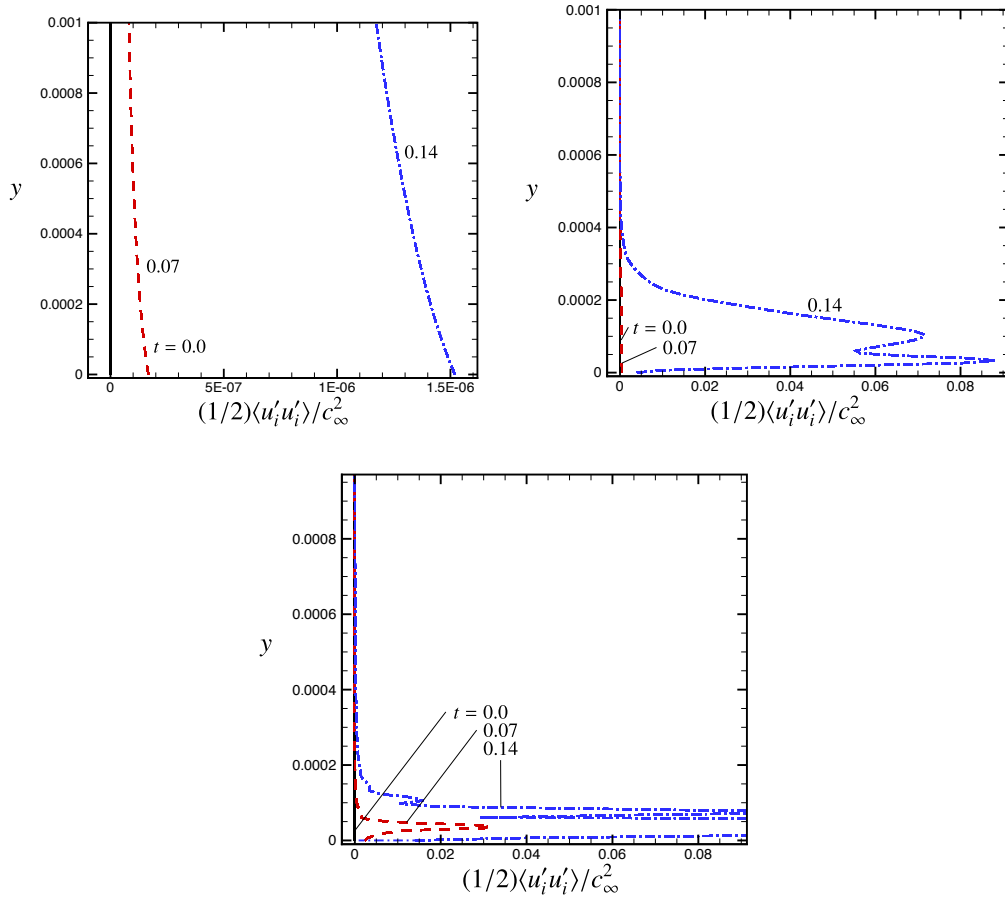


FIGURE 6. Evolution of the disturbance turbulent kinetic energy for the three different mean flows. Upper left: uniform, steady; Upper right: nonuniform, steady; Bottom: nonuniform, unsteady.

turbances exist implying that the panel-induced modification to the turbulence may be inhomogeneous over the scale of a vehicle where the local boundary layer thickness varies.

Global statements are not yet possible but it appears clear that a turbulent boundary layer can, indeed, be modified by the panel motion and that the modification levels are dependent on the boundary layer thickness as it can couple to the panel motion. The strong baseflow dependence implies that simplified theories will need to account for boundary layer growth in the spatially-developing case and that the amplitudes seen in Figure 6 suggest that nonlinearities may be important for long time estimates to be realistic.

## 5. Conclusions

A linearized analysis of the disturbances induced by a compliant surface was performed. The surface motion predicted from a fully coupled direct numerical simulation of a Mach 2.25 boundary layer that underwent laminar-to-turbulent transition was extracted and used as input for a linearized Navier-Stokes calculation about three different baseflows.

The baseflows were characterized as being steady and uniform, steady and nonuniform, and unsteady and nonuniform. The nonuniform baseflows used the mean profiles extracted from a complementary direct numerical simulation of a Mach 2.25 boundary layer over a rigid surface. The linearized calculations demonstrate that the grazing boundary layer has a very strong influence on the amplification of the panel-induced disturbances and can act as a selective amplifier whose gains change along with the boundary layer growth. The assumption of a uniform and steady mean does not appear to be appropriate for modeling how boundary motion can induce flow disturbances. The nonuniform mean flows exhibited much larger amplification, compared with the uniform case, but also demonstrated sensitivity to the thickness of the boundary layer. These results suggest that not only is modification of the turbulent structure possible but its impact on a spatially developing boundary layer will be spatially varying and, as was seen in the steady but nonuniform mean flow case, disturbance amplification may be sufficient to cause boundary layer transition.

#### Acknowledgments

This work was originally supported by the U.S. Air Force Research Laboratory Air Vehicles Directorate under Contract No. FA8650-06-2-3620. Input from Dr. S. M. Spottswood, our technical monitor, at AFRL (Wright-Patterson AFB) is gratefully acknowledged. Computational resources were provided by the DOD Distributed Shared Research Centers at ERDC, ARL, and NAVO. Continuing support by the Air Force Office of Scientific Research under Contract No. FA9550-14-1-0101, with Dr. “Pon” R. Ponnappan as technical monitor, is gratefully acknowledged.

#### REFERENCES

- BEBERNISS, T., SPOTTSWOOD, M. & EASON, T. 2011 High-speed digital image correlation measurements of random nonlinear dynamic response. In *Exp. and Appl. Mech.* (ed. T. Proulx), vol. 6, pp. 171–186. Springer.
- DOWELL, E. H. 1970 Panel flutter: a review of the aeroelastic stability of plates and shells. *AIAA J.* **8** (3), 385–399.
- EKOTO, I. W., BOWERSOX, R. D. W., BEUTNER, T. & GOSS, L. 2008 Supersonic boundary layers with periodic surface roughness. *AIAA J.* **46** (2), 486–497.
- EKOTO, I. W., BOWERSOX, R. D. W., BEUTNER, T. & GOSS, L. 2009 Response of supersonic turbulent boundary layers to local and global mechanical distortions. *J. Fluid Mech.* **630**, 225–265.
- GLASS, C. E. & HUNT, L. R. 1986 Aerothermal tests of spherical dome protuberances on a flat plate at a Mach number of 6.5. Technical Paper no. 2631, NASA.
- GLASS, C. E. & HUNT, L. R. 1988 *Aerothermal tests of quilted dome models on a flat plate at a Mach number of 6.5*. NASA Technical Report no. TP-2804, NASA Langley Research Center.
- JACOBI, I. & MCKEON, B. J. 2011a Dynamic roughness perturbation of a turbulent boundary layer. *J. Fluid Mech.* **688**, 258–296.
- JACOBI, I. & MCKEON, B. J. 2011b New perspectives on the impulsive roughness-perturbation of a turbulent boundary layer. *J. Fluid Mech.* **677**, 179–203.
- MCKEON, B. J., SHARMA, A. S. & JACOBI, I. 2013 Experimental manipulation of wall turbulence: A systems approach. *Phys. Fluids*, **677** 031301.
- NATARAJAN, M., FREUND, J. B. & BODONY, D. J. 2014 Actuator and sensor placement

for flow control. AIAA Paper 2014-2100, Presented at the 7th AIAA Flow Control Conference, Atlanta, GA.

- OSTOICH, C., BODONY, D. J. & GEUBELLE, P. H. 2013 Interaction of a Mach 2.25 turbulent boundary layer with a fluttering panel using direct numerical simulation. *Phys. Fluids* **25**, 110806).
- STRAND, B. 1994 Summation by parts for finite difference approximations for  $d/dx$ . *J. Comput. Phys* **110**, 47–67.
- SVÄRD, M., CARPENTER, M. H. & NORDSTRÖM, J. 2007 A stable high-order finite difference scheme for the compressible Navier-Stokes equations, far-field boundary conditions. *J. Comput. Phys.* **225**, 1020–1038.
- SVÄRD, M. & NORDSTRÖM, J. 2008 A stable high-order finite difference scheme for the compressible Navier-Stokes equations: No-slip wall boundary conditions. *J. Comput. Phys.* **227**, 4805–4824.
- VISBAL, M. R. & GAITONDE, D. V. 2002 On the Use of Higher-Order Finite-Difference Schemes on Curvilinear and Deforming Meshes. *J. Comput. Phys.* **181**, 155–185.